

Promotion of *n*-Butane Isomerization Activity by Hydration of Sulfated Zirconia

Martín R. González, Jeffrey M. Kobe, Kevin B. Fogash, and James A. Dumesic¹

Department of Chemical Engineering, University of Wisconsin, Madison, Wisconsin 53706

Received October 5, 1995; revised December 27, 1995; accepted January 4, 1996

Microcalorimetry and infrared spectroscopy were used in conjunction with reaction kinetics measurements to investigate the effects of catalyst hydration on the activity for *n*-butane isomerization at 423 K of sulfated zirconia. The catalytic activity for a sample dried at 773 K is an order of magnitude lower than that of a sample dried at 588 K. However, the catalytic activity for the sample dried at 773 K is promoted by dosing quantities of water equal to approximately 75 $\mu\text{mol/g}$ onto the surface at 423 K. Larger doses of water poison the catalyst. The acidity of the catalyst after drying at either 588 or 773 K was almost entirely of the Brønsted acid type. Dehydration of the catalyst did not alter the heat or the extent of ammonia adsorption. Water dissociates upon adsorption on the sample dried at 773 K, producing new hydroxyl groups whose presence is critical for *n*-butane isomerization on sulfated zirconia.

© 1996 Academic Press, Inc.

INTRODUCTION

The isomerization of straight-chain paraffins to more highly branched species is beneficial for the production of cleaner-burning fuels. For example, *n*-butane, which is undesirable for gasoline, may be converted to isobutane, a valuable precursor to MTBE and other fuel additives. The technology currently used for butane isomerization is based on air-sensitive catalysts (1) that operate at elevated temperatures where the equilibrium conversion to branched isomers is not favorable (2).

Paraffin isomerization is believed to proceed through carbenium ion chemistry, which requires the presence of strong Brønsted acid sites (3). Several researchers have found evidence of unusually strong acidity on sulfated zirconia catalysts, denoted as "superacidity" (4–9). These catalysts are active for *n*-butane isomerization at lower temperatures (e.g., 370 K) than conventional isomerization catalysts (e.g., 470 K). Brønsted acidity is commonly observed on these sulfated zirconia catalysts, although strong Lewis acidity has also been implicated in the high reactivity of these materials (6, 10–19). Furthermore, some researchers have suggested

that the combination of Lewis and Brønsted acid sites on sulfated zirconia catalysts is necessary to achieve alkane conversion at low temperatures (6, 11, 17–19).

Investigations of the acidity of sulfated zirconia catalysts are complicated by the sensitivity of these materials to preparation conditions (6, 11, 17, 18, 20–28). For example, the temperature at which the catalyst is dried after calcination and exposure to atmospheric moisture is extremely important in determining catalytic activity (12, 18, 22, 23, 28, 29). In addition, various authors have found in spectroscopic studies of adsorbed basic probe molecules that water transforms the Lewis acid sites of sulfated zirconia into Brønsted acid sites (11, 12, 14, 18, 22, 23). Nevertheless, the effects of adsorbed water on the activity of sulfated zirconia for *n*-butane isomerization are ambiguous, since water has been identified as both a promoter (23) and a poison (30, 31).

In the present study, *n*-butane isomerization is carried out over a sulfated zirconia catalyst prepared in two states of dehydration. Infrared spectroscopy of adsorbed ammonia is used to determine the nature of the acid sites present on the catalyst, while the strength distribution of the acid sites is assessed using ammonia adsorption calorimetry. The promotional effect of adsorbed water on the isomerization activity of sulfated zirconia is then investigated. Water adsorption calorimetry is employed to examine the hydroscopic nature of the catalyst, and infrared spectra are collected for the catalyst at varying degrees of hydration.

EXPERIMENTAL

The sulfated zirconia catalysts used in this study were prepared from sulfuric acid-treated zirconium hydroxide provided by MEI Corporation. This precursor was heated in flowing oxygen (100 $\text{cm}^3/\text{g} \cdot \text{min}$, NPT) from room temperature to 848 K over a period of 1.5 h. After calcination for 2 h at this temperature, the catalyst was transferred in air to a vial and stored in a desiccator. The calcined material contains 1.8% sulfur by weight, as determined by chemical analysis (Galbraith Laboratories). The BET surface area after this treatment is 98 m^2/g . Prior to subsequent

¹ To whom correspondence should be addressed.

experimental studies, the catalyst was dried for 1 h in flowing He ($65 \text{ cm}^3/\text{min}$, NPT) at either 588 or 773 K to study the effect of moisture content. The material dehydrated at 588 K is designated as MEI-1 and the sample dried at 773 K is denoted as MEI-2.

Experiments involving adsorption of pyridine, ammonia, or water were conducted with the sulfated zirconia samples maintained at 423 K during initial exposure. All probe molecules were purified before use by successive freeze-pump-thaw cycles. Ammonia was kept under a dry ice/acetone bath during use to remove moisture. Molecular sieves (13X, Davison) were used to remove moisture from pyridine.

The isomerization of *n*-butane was carried out on catalysts MEI-1 and MEI-2 at 423 K using a gas composition of 10% *n*-butane (AGA, 99.5% purity, instrument grade) in He (Liquid Carbonic). A quartz flow reactor, 1.27 cm in diameter, was loaded with approximately 0.2 g of catalyst and 0.1 g of quartz particles. This solid mixture was dried in flowing He ($65 \text{ cm}^3/\text{min}$) for 1 h at 588 K (MEI-1) or 773 K (MEI-2). For the hydration experiments, the catalyst was dried at 773 K before adsorption of the indicated amount of water at 423 K.

Helium and *n*-butane were purified by oxygen-absorbent traps (Alltech), and water impurities were removed by molecular sieve traps (13X) at 77 K and at room temperature for He and *n*-butane, respectively. Reaction products were analyzed using a Hewlett-Packard 5890 gas chromatograph equipped with a flame ionization detector. The chromatograph contained a 7.3-m 5% DC-200 Chromosorb P-AW column held at 323 K. Activities and selectivities are calculated on the basis of hydrocarbon products detected in the reactor effluent. Initial activity measurements were taken at 3 min on stream.

Infrared spectra of adsorbed ammonia were collected at room temperature using a Mattson Galaxy 5020 FTIR spectrometer. Samples were pressed into self-supporting pellets ($18 \text{ mg}/\text{cm}^2$) at a pressure of $\sim 70 \text{ MPa}$. Drying was performed under vacuum (10^{-4} Pa) in a cell containing CaF_2 windows. Samples were dried for 1 h at 588 K (MEI-1) or 773 K (MEI-2). During the adsorption of ammonia or water, the catalyst pellet was maintained at 423 K. All spectra were collected at room temperature at a resolution of 8 cm^{-1} .

Microcalorimetric studies of the adsorption of ammonia and water were performed at 423 K using a Tian-Calvet type heat-flux calorimeter connected to a gas-handling system. A volumetric system equipped with a Baratron capacitance manometer was used for precision pressure measurements. The design and operation of this apparatus have been described elsewhere (32). Samples weighing approximately 0.6 g were pelletized and evacuated to 10^{-4} Pa at 588 K (MEI-1) or 773 K (MEI-2) for 1 h. The samples were then allowed to equilibrate overnight in the heat sink at 423 K

under 30–55 kPa of argon before calorimetric measurements were taken. Differential heats of adsorption versus adsorbate coverage were obtained by measuring the energy evolved from sequential doses of the adsorbate gas (2–10 μmol) onto the catalyst. In all cases, the enthalpy change associated with adsorption of the probe molecule is exothermic, and the heat of adsorption reported in the current study is defined as the absolute value of this quantity.

RESULTS

Figure 1 shows the catalytic activity for *n*-butane isomerization of sulfated zirconia dried at 588 K and at 773 K. The initial activity of the catalyst dried at the lower temperature (MEI-1) is about $2.10 \mu\text{mol}/\text{g} \cdot \text{s}$. The activity decreases with time as the catalyst deactivates due, at least in part, to the formation of coke (33). Some reduction of sulfur may also take place (34, 35). The selectivity of this catalyst for isomerization to isobutane is 92%, with the balance of the products consisting mainly of propane and isopentane.

In contrast to the MEI-1 sample, the catalyst dried at the higher temperature (MEI-2) shows low activity, initially isomerizing *n*-butane at a rate of $0.12 \mu\text{mol}/\text{g} \cdot \text{s}$. The selectivity of this catalyst for isomerization is about 80%. After 1 h on stream, no measurable conversion of *n*-butane takes place over MEI-2. A detailed discussion of the reaction kinetics is given elsewhere (36).

To investigate the nature of the acid sites present on the MEI-1 and MEI-2 samples, infrared spectroscopy was performed prior to and following the adsorption of ammonia. Figure 2A shows infrared spectra of the MEI-1 and MEI-2 sulfated zirconia samples. Both spectra show strong absorbance in the range $1300\text{--}1420 \text{ cm}^{-1}$, characteristic of SO_4 groups on the surface of metal oxides. Some authors have assigned the band at 1400 cm^{-1} to the asymmetric S=O stretching mode of sulfate groups bound by two bridging oxygen atoms to the surface (12, 22, 23, 37, 38). However,

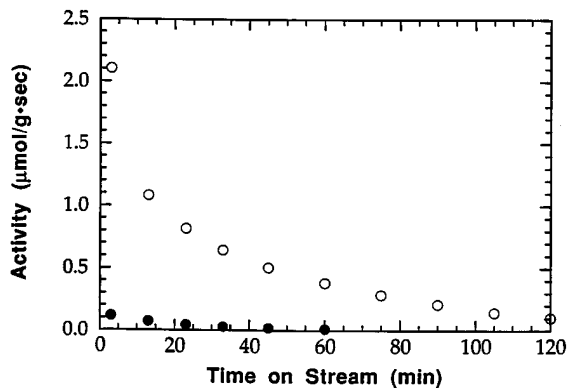


FIG. 1. Rate of *n*-butane isomerization at 423 K versus time on stream over sulfated zirconia dried at 588 K (○) and at 773 K (●).

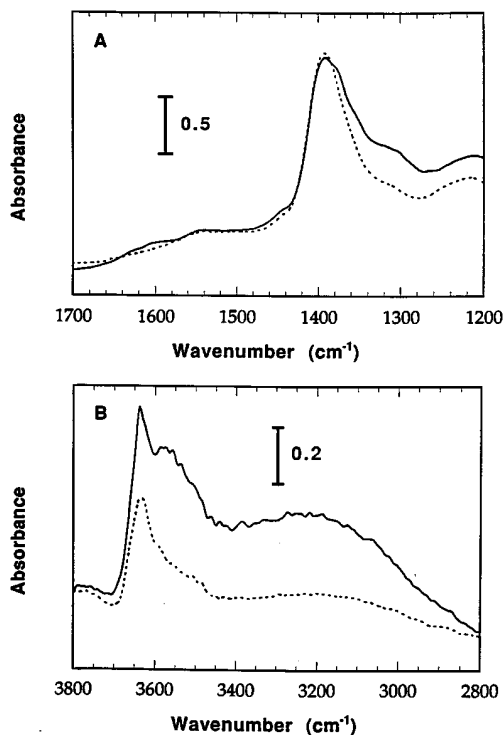


FIG. 2. Infrared spectra of sulfated zirconia dried at 588 K (solid line) and at 773 K (broken line), showing S=O stretching region (A) and O-H stretching region (B). Absorbance scales are provided in the figure.

an accurate representation of the sulfate group is difficult to determine, partly because this S=O stretching of sulfated metal oxides occurs at least 100 cm^{-1} higher than that expected for inorganic sulfates (39, 40). The number of S=O double bonds present in a single sulfate group is determined in other materials by counting the number of bands due to a single vibrational mode. For example, the bidentate species mentioned above should exhibit three bands due to the asymmetric S=O stretching mode, and three bands due to the symmetric mode, that would appear between 1000 and 1200 cm^{-1} (39, 41). An unidentate species should exhibit two bands due to each of these modes. The absence of bands near 1200 cm^{-1} has prompted some researchers (29, 38) to suggest the presence of species containing only one S=O bond, the other three bonds of sulfur being bridging oxygen bonds to zirconium or to the sulfur of another sulfate group. The spectra of the current work show broad features near 1200 cm^{-1} , which do not conclusively disclose the nature of the sulfate species present. It should be noted that the presence of fewer than two S=O bonds implies that sulfur has been reduced from the +6 oxidation state during sample preparation.

The sample dried at the lower temperature, MEI-1, exhibits much of its S=O stretching at relatively low frequencies, near 1300 cm^{-1} . Although this may be interpreted as a sign of adsorbed species on this sample, there is essentially

no difference between the MEI-1 and MEI-2 samples in the 1200 – 1800 cm^{-1} spectral region. Conspicuously absent from the spectrum of MEI-1 is the H–O–H bending band at 1630 cm^{-1} which would be observed in the presence of molecularly adsorbed water (42, 43).

Spectra of the hydroxyl-stretching region of the catalysts are displayed in Fig. 2B. In agreement with other spectroscopic studies of sulfated zirconia (29, 37, 42, 44), the strongest absorbance for both samples is seen at 3640 cm^{-1} . The intensity of this sharp band is slightly higher on MEI-1 than on MEI-2. In addition to absorbance at this frequency, MEI-1 shows two regions of hydroxyl stretching absorbance at lower wavenumbers: a broader band centered at approximately 3550 cm^{-1} and an extremely broad region extending from 2800 to 3400 cm^{-1} . These features are indicative of surface OH groups that are strongly hydrogen bonded to each other or to other groups on the surface (43). Thus, the surface of the catalyst dehydrated at 588 K is populated by hydroxyl groups that are removed by the more severe drying treatment at 773 K . The presence of additional hydroxyl groups on the sample dried at the lower temperature is not surprising and is consistent with the possibility of a higher concentration of Brønsted acid sites.

Infrared spectra of ammonia adsorbed in small increments on MEI-1 (μmol of NH_3 per gram of catalyst) are presented in Fig. 3. As reported elsewhere (45), this catalyst contains almost exclusively Brønsted acid sites, evidenced by the band near 1440 cm^{-1} , which grows as ammonia is added. Moreover, the first $5\text{ }\mu\text{mol/g}$ of ammonia adsorbed on MEI-1 cause the appearance of a weak band at 1600 cm^{-1} , whose intensity does not change with increasing coverage. This absorbance, tentatively assigned to coordinatively bound NH_3 , suggests that there are fewer than $5\text{ }\mu\text{mol/g}$ of Lewis acid sites on the catalyst (45).

With increasing uptake of the ammonia probe molecule, intensity in the region 1370 – 1420 cm^{-1} diminishes, while

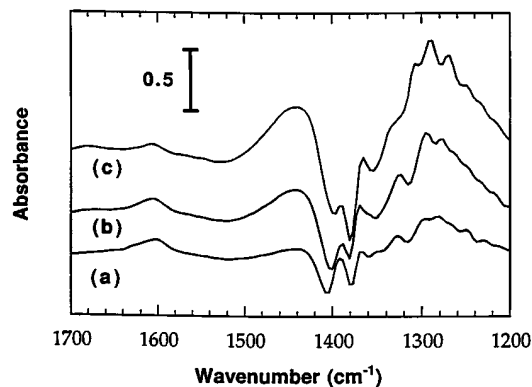


FIG. 3. Infrared spectra of NH_3 adsorbed on MEI-1 at coverages of $5\text{ }\mu\text{mol/g}$ (a), $27\text{ }\mu\text{mol/g}$ (b), and $55\text{ }\mu\text{mol/g}$ (c). The absorbance of the clean sample dried at 588 K has been subtracted from all spectra. Absorbance scale is provided in the figure.

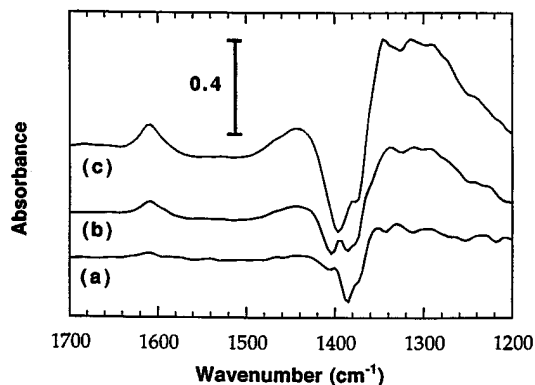


FIG. 4. Infrared spectra of NH_3 adsorbed on MEI-2 at coverages of $5 \mu\text{mol/g}$ (a), $25 \mu\text{mol/g}$ (b), and $50 \mu\text{mol/g}$ (c). The absorbance of the clean sample dried at 773 K has been subtracted from all spectra. Absorbance scale is provided in the figure.

that at 1280 cm^{-1} increases. This apparent shift of $\text{S}=\text{O}$ stretching absorbance to lower frequencies is related to a withdrawal of electrons by adsorbed molecules (16, 23, 38). Two different bands in the $\text{S}=\text{O}$ stretching range are seen to shift upon ammonia adsorption, suggesting that the catalyst may contain the unidentate sulfate species described above. Alternatively, these two frequencies of $\text{S}=\text{O}$ stretching may belong to different types of sulfate species. At least three different species possessing $\text{S}=\text{O}$ double bonds have been differentiated spectroscopically on sulfated zirconia (12, 22, 29, 38).

Figure 4 shows difference spectra of ammonia adsorbed incrementally on MEI-2. Again, the $\text{S}=\text{O}$ asymmetric stretching in the range $1370\text{--}1420 \text{ cm}^{-1}$ shifts to lower frequencies as increasing amounts of ammonia are adsorbed. As with MEI-1, more than one type of sulfate species is evidently involved in the interaction with ammonia.

Bands at 1440 and 1600 cm^{-1} appear upon addition of the first $5 \mu\text{mol/g}$ of ammonia, indicating the presence of Brønsted and Lewis acid sites on the MEI-2 sample. Unlike the MEI-1 sample, the band due to coordinatively bound ammonia continues to grow on MEI-2 with increasing ammonia uptake. Thus, the Lewis sites of the MEI-2 catalyst are not confined to the strongest $5 \mu\text{mol/g}$ of acid sites. The existence of both Brønsted and Lewis acid sites on MEI-2 is more clearly displayed in the difference spectrum of adsorbed pyridine (Fig. 5). The most commonly used bands for identification of pyridine adsorbed on Lewis and Brønsted acid sites are those at 1450 and 1550 cm^{-1} , respectively.

An important result is revealed in Fig. 6 by examining the relative intensities of the bands due to adsorbed ammonia on MEI-1 and MEI-2 at $50 \mu\text{mol/g}$ NH_3 coverage. The absorbance at 1600 cm^{-1} , assigned to Lewis acid-bound ammonia, is approximately the same on both samples. However, the intensity of the 1440 cm^{-1} band, due to ammonium ions associated with Brønsted acid sites, is

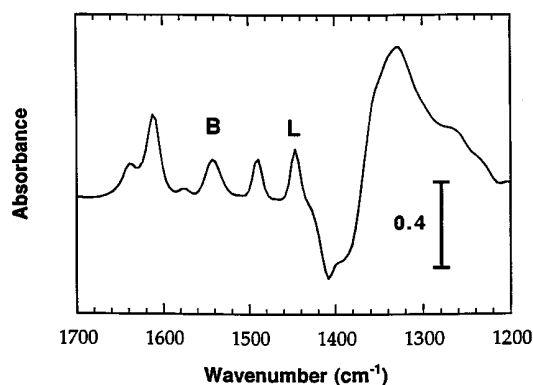


FIG. 5. Infrared spectrum of $104 \mu\text{mol/g}$ pyridine adsorbed on MEI-2, with absorbance due to the clean sample subtracted. "B" and "L" denote bands due to pyridine bound to Brønsted and to Lewis acid sites, respectively. Absorbance scale is provided in the figure.

significantly greater on MEI-1 than on MEI-2. Since the catalysts contain approximately equal amounts of adsorbed ammonia, any increase in absorbance at 1440 cm^{-1} should be accompanied by a decrease in absorbance at 1600 cm^{-1} . These changes would indicate the conversion of Lewis acid sites to Brønsted sites such as observed in the pyridine adsorption spectra of other authors (12, 18, 23, 30). No such transformation is apparent here. Rather, it appears that the extinction coefficients of ammonium ions on the surface of sulfated zirconia increase with the degree of hydration of the catalyst.

Differential heats of ammonia adsorption at 423 K versus adsorbate coverage are shown in Fig. 7 for the MEI-1 and MEI-2 catalysts. Microcalorimetric data for ammonia adsorption on MEI-1 have been previously reported (45). The two samples of the present study show essentially the same behavior for differential heats of ammonia adsorption to a coverage of $100 \mu\text{mol/g}$. Both catalysts contain

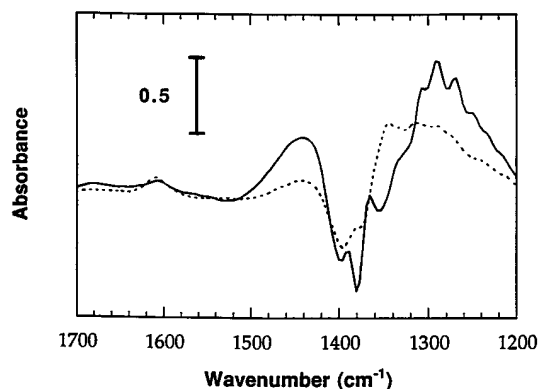


FIG. 6. Difference infrared spectra of NH_3 adsorbed on MEI-1 (solid line) and MEI-2 (broken line) at coverages of 55 and $50 \mu\text{mol/g}$, respectively. This is the same information provided in curves (c) of Figs. 3 and 4. Absorbance scale is provided in the figure.

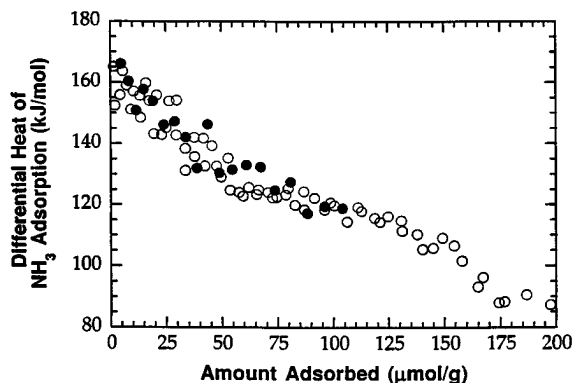


FIG. 7. Differential heat of NH_3 adsorption versus adsorbate coverage at 423 K on MEI-1 (○) and MEI-2 (●).

approximately $50 \mu\text{mol/g}$ of strong acid sites having differential heats of ammonia adsorption in the range of 125–165 kJ/mol. Also evident on both samples is a group of about $50 \mu\text{mol/g}$ of sites giving differential heats of ammonia adsorption equal to 115–125 kJ/mol. Beyond these first $100 \mu\text{mol/g}$ of acid sites, at least $100 \mu\text{mol/g}$ of sites are present whose interaction with ammonia is characterized by the release of less than 115 kJ/mol. These weaker sites are of little catalytic importance, since the activity for isomerization is eliminated after the first $70 \mu\text{mol/g}$ of sites are poisoned by adsorbed ammonia (46). It should be noted that the MEI samples of this study contain $560 \mu\text{mol/g}$ of sulfur, and $1 \mu\text{mol/g}$ corresponds to 6×10^{15} sites/ m^2 .

Figure 7 demonstrates that the differential heat of ammonia adsorption versus ammonia coverage is insensitive to the temperature of vacuum dehydration within the range 588–773 K. Thus, a simple consideration of acid strength, as measured by the heat of ammonia adsorption, cannot account for the significant difference in the *n*-butane isomerization activity displayed by the catalysts dried at these two temperatures.

Figure 8 shows the differential heats of ammonia and water adsorbed in succession on MEI-2. These data indicate that the heat of ammonia adsorption on MEI-2 remains unchanged after the adsorption of $105 \mu\text{mol/g}$ of water. Conversely, heats of water adsorption on MEI-2 are unaffected by the presence of $104 \mu\text{mol/g}$ of preadsorbed ammonia. Moreover, the differential heats of adsorption of these two probe molecules on MEI-2 exhibit the same trends with surface coverage. This behavior suggests that the sites to which ammonia and water adsorb are closely related, yet not the same sites as preadsorption of one species does not block adsorption of the other species.

The heats of ammonia adsorption are similar to those observed for ammonia on other acidic oxide catalysts (47). The decreasing heat of adsorption with increasing coverage strongly suggests that sufficient mobility is achieved at 423 K to allow equilibration of the probe molecules with the

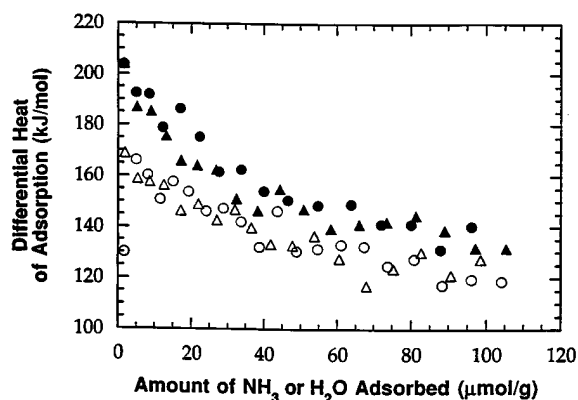


FIG. 8. Differential heats of NH_3 and H_2O adsorption versus adsorbate coverage at 423 K on MEI-2. Two calorimetric experiments are shown in which: (1) incremental adsorption of $104 \mu\text{mol/g}$ of NH_3 (○) is followed by adsorption of $96 \mu\text{mol/g}$ of H_2O (●) and (2) adsorption of $105 \mu\text{mol/g}$ of H_2O (▲) is followed by $99 \mu\text{mol/g}$ of NH_3 (△).

catalyst (47). Thus, for the rehydration kinetics experiments performed in a similar manner, the dosed water should retain sufficient mobility for equilibration with the catalyst at 423 K.

The data of Fig. 8 indicate that the heat of water adsorption on MEI-2 is higher than that of ammonia adsorption for at least the first $100 \mu\text{mol/g}$ of adsorbed species. Because water is a weaker base than ammonia, the high differential heat of adsorption suggests that water probably dissociates on the surface, for example, by interacting with bridging oxygens to form new hydroxyl groups on the surface (48, 49). This conclusion is consistent with the higher OH concentration displayed by the MEI-1 sample in the infrared spectra of Fig. 2.

To investigate the effect of surface water content on the catalytic activity for *n*-butane isomerization activity, the MEI-2 sample was rehydrated incrementally with known quantities of water that were chosen with respect to the differential heat of water adsorption versus adsorbate coverage determined calorimetrically. In particular, a plot of the differential heat of water adsorption on MEI-2 is shown in Fig. 9. The initial heat of water adsorption is approximately 205 kJ/mol, although several groups of sites are discernible which display varying strengths of interaction with the surface.

The first $25 \mu\text{mol/g}$ of sites adsorb water with differential heats of 160–205 kJ/mol. The next $25 \mu\text{mol/g}$ of sites exhibit differential heats of 145–160 kJ/mol. At a heat of 140 kJ/mol, a plateau of approximately $25 \mu\text{mol/g}$ can be distinguished, followed by $25 \mu\text{mol/g}$ of sites with heats of water adsorption in the range 125–135 kJ/mol. Finally, an additional $50 \mu\text{mol/g}$ of sites are characterized by a differential heat of water adsorption of 110–125 kJ/mol. Based on this behavior of differential heat of water adsorption versus adsorbate coverage, reaction kinetics experiments and infrared spectroscopy were performed on formulations

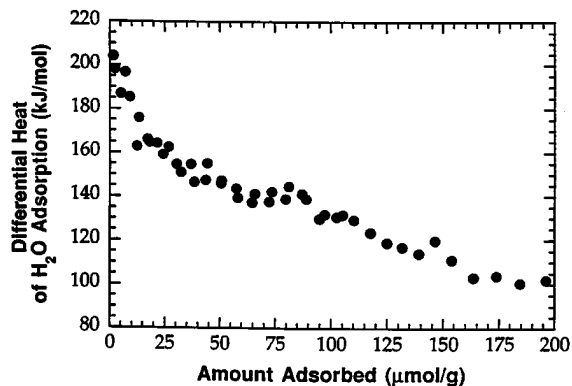


FIG. 9. Differential heat of H₂O adsorption versus adsorbate coverage at 423 K on MEI-2.

of MEI-2 titrated with approximately 25, 50, 75, 100, and 150 μmol/g of water.

Figure 10 shows the initial rate of *n*-butane isomerization for each of the rehydrated catalysts. As described above, the *n*-butane isomerization activity of MEI-2 at 3 min on stream is 0.12 μmol/g · s, while the activity of MEI-1 is 2.10 μmol/g · s. Adding 24 μmol/g of H₂O to MEI-2 causes a significant increase in catalytic activity to a value of approximately 0.80 μmol/g · s. The promotional effect of water addition to MEI-2 continues until a maximum catalytic activity of 1.46 μmol/g · s is reached upon addition of 74 μmol/g H₂O. Water acts as a poison at higher amounts on the catalyst. For example, the initial catalytic activity for *n*-butane conversion over MEI-2 after treatment with 146 μmol/g of water is only slightly higher than that of the original dehydrated catalyst.

Infrared spectra of the MEI-2 catalyst rehydrated with different amounts of water are shown in Fig. 11A. A weak band grows at 1600 cm⁻¹ with increasing hydration. This band is assigned to the overtone of an OH bending mode present at about 800 cm⁻¹, and it is probably associated with the hydroxyl stretching observed at 3640 cm⁻¹. Such

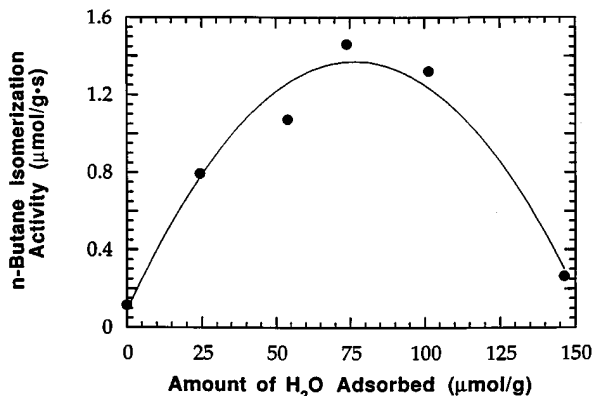


FIG. 10. Initial rate of *n*-butane isomerization at 423 K versus amount of H₂O adsorbed on MEI-2. All activities are calculated at 3 min on stream.

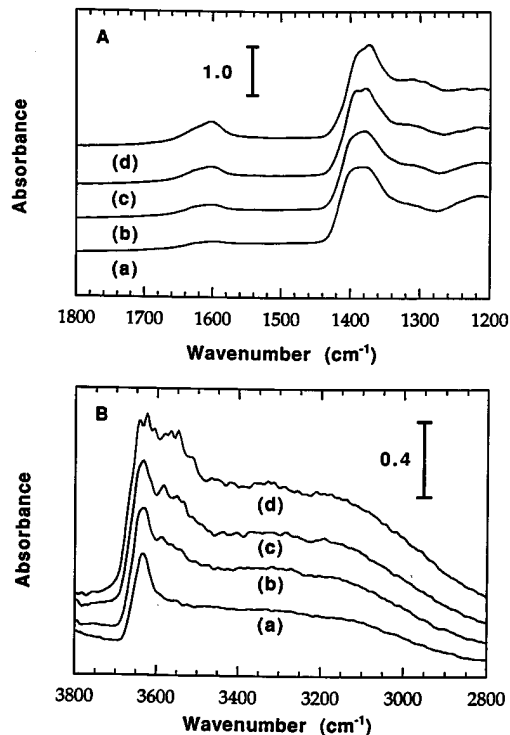


FIG. 11. Infrared spectra of H₂O adsorbed on MEI-2 at coverages of 0 μmol/g (a), 26 μmol/g (b), 51 μmol/g (c), and 102 μmol/g (d), showing S=O stretching region (A) and O-H stretching region (B). Absorbance scales are provided in the figure.

an overtone would be expected to appear when an adsorbed polar molecule introduces anharmonicity into the original bending vibration (50). Since our calorimetric results suggest that water adsorbs dissociatively on MEI-2 for the coverages of this study, the band at 1600 cm⁻¹ cannot be caused by the H-O-H scissors-deformation of molecular water, which shows absorbance at 1630 cm⁻¹ (43). The asymmetric S=O stretching of the sulfate groups shifts to lower frequencies as the water uptake increases.

Figure 11B displays the OH stretching region of MEI-2 at various stages of sample rehydration. As water is added to the catalyst, the spectrum becomes more similar to that of MEI-1. The intensity of the OH band at 3640 cm⁻¹ increases and a new, broader band centered at 3550 cm⁻¹ appears. In addition, the absorbance of the entire region extending from 2800 to 3400 cm⁻¹ increases. The new bands of the rehydroxylated MEI-2, however, are not as clearly defined as for the MEI-1 sample. This slight difference may indicate that the newly formed OH groups on MEI-2 by rehydroxylation may have a greater tendency toward hydrogen bonding than the OH groups on MEI-1.

DISCUSSION

The adsorption of large amounts of water onto sulfated zirconia has been shown in the literature to poison *n*-butane

isomerization (30, 31). However, the results of the present study indicate that water promotes *n*-butane isomerization over sulfated zirconia for moderate extents of catalyst hydration.

The results of Fig. 1 show that a sample dehydrated at 773 K (MEI-2) exhibits an initial activity for isomerization that is an order of magnitude lower than that of a sample dried at 588 K (MEI-1). Gravimetric measurements reported elsewhere (36) indicate that this increase in drying temperature leads to the removal of about 110 $\mu\text{mol/g}$ of water from the catalyst. As seen in Fig. 10, the maximum rate of *n*-butane conversion observed during rehydration of the MEI-2 sample occurs for 74 $\mu\text{mol/g}$ of H_2O , which corresponds to 67% rehydration of the catalyst. This treatment restores approximately 70% of the activity lost in the drying process at 773 K. The portion of the activity which is not regained may indicate that some of the dehydroxylation which occurs at 773 K is irreversible. For example, metal oxides dehydrated at high temperatures may possess annealed oxygen bridges which are rehydrated only by immersion in liquid water (43).

It is interesting to note some similarities observed in the present study upon rehydration of sulfated zirconia with results reported in the literature for a series of silica–alumina catalysts. Specifically, Mills and co-workers (51) found that the adsorption of water on a silica–alumina catalyst dried at 798 K promoted the activity for isomerization of 2-methylpentane. The activity of this catalyst passed through a maximum when a quantity of H_2O was added equal to 0.05 wt% ($\sim 25 \mu\text{mol/g}$). In addition, Haldeman and Emmett (52) reported that the rate of deuterium exchange between isobutane and a deuterated silica–alumina catalyst was dependent on the amount of D_2O adsorbed. The authors concluded that preadsorbed water “activated” the adsorption of isobutane on silica–alumina (52), although it did not alter the amount of adsorbed isobutane (53).

From the similarities that can be drawn between sulfated zirconia and silica–alumina, we suggest that the promotional effect of water does not result entirely from the presence of sulfur in the catalyst. This suggestion is consistent with the finding that sulfated zirconia exhibits heats of water adsorption comparable to those of zirconia containing no sulfate (54).

While the catalytic activity of MEI-1 is significantly higher than that of MEI-2, the results in Fig. 7 indicate that the differential heat of ammonia adsorption is not related directly to the *n*-butane isomerization activity. Microcalorimetric measurements of ammonia adsorption have been successfully correlated with the acid strengths of silica–alumina (55) and H-ZSM-5 (56). However, Gorte and co-workers (57) have recently suggested that the differential heat of ammonia adsorption may not be a reliable measure of acid strength, since this heat has contributions from acidic

as well as nonacidic interactions, i.e., the proton affinity of the acid site and the stabilization of the acid–base adduct on the surface, respectively.

The absence of a correlation between the heat of ammonia adsorption and the catalytic activity for the isomerization of *n*-butane over sulfated zirconia may also suggest that this reaction is not strictly acid-catalyzed. This idea has been proposed by Gates and co-workers (58), who compared the products of *n*-butane reaction over iron- and manganese-promoted sulfated zirconia with those formed over H-ZSM-5. We suggest that the presence of acid sites is a necessary but not a sufficient condition for high catalytic activity for *n*-butane isomerization at the reaction conditions of the present study. In particular, this reaction over MEI-1 is effectively eliminated after the strongest 70 $\mu\text{mol/g}$ of acid sites have been neutralized with ammonia (46); however, the MEI-2 sample shows low activity even though it possesses strong acid sites. Further, adsorption of butane on the surface sulfate species could involve an oxidation–reduction process, as suggested by TPD studies of bases on modified sulfated zirconia catalysts which revealed the presence of oxidized adsorbed species (59–61).

The infrared spectra of ammonia adsorbed on MEI-1 (Fig. 3) and MEI-2 (Fig. 4) reveal that a majority of the strongest 50 $\mu\text{mol/g}$ of acid sites on both catalysts are Brønsted acid sites, although the pyridine adsorption spectrum of Fig. 5 indicates the presence of some Lewis acid sites. The conversion of Lewis acid sites to Brønsted acid sites by adsorbed water has been reported by various authors who have collected infrared spectra of adsorbed pyridine on sulfated zirconia (12, 18, 23, 30). These researchers speculate that the observed transformation leads to an enhancement in isomerization activity, and one author has attributed a loss of activity to this effect (14). In contrast, Corma *et al.* (13) suggest that the infrared spectrum of adsorbed pyridine is not a reliable method for determining the nature of the acid sites of sulfated zirconia, because the deformation modes assigned to pyridine on H-mordenite and sulfated zirconia do not correlate well with the observed *n*-butane isomerization activity.

As discussed elsewhere (62), the intensity of the 1440 cm^{-1} band of ammonia adsorbed on MEI-2 increases as water is added. Thus, the conversion of Lewis sites to Brønsted sites that may occur under certain circumstances is difficult to quantify due to changes in the extinction coefficients of adsorbed probe molecules. A related effect was observed in the ^{31}P NMR spectra obtained by Lunsford (11), who reported that the conversion of Lewis to Brønsted acid sites is not stoichiometric with water addition.

Figure 6 shows that although MEI-1 exhibits a greater absorbance at 1440 cm^{-1} (due to ammonia adsorbed on Brønsted acid sites) compared to MEI-2, the absorbance at 1600 cm^{-1} (due to ammonia on Lewis acid sites) is approx-

imately the same on both samples. Based on these data, a significant conversion of Brønsted acid sites to Lewis acid sites does not appear to take place upon dehydration. This result is supported by calorimetric experiments involving CO adsorption (54), which suggest that MEI-1 and MEI-2 contain the same strength and number of Lewis acid sites.

Ammonia and water both produce an increase in absorbance at 1600 cm^{-1} when adsorbed on sulfated zirconia. It should be noted that a band at this frequency appears on the catalyst in adsorption experiments, regardless of the drying temperature or the identity of the probe molecule (54). Therefore, this band is likely due to some feature of the catalyst surface and not to an adsorbed species. The most plausible assignment for such a band is the overtone of an OH bending mode occurring at about 800 cm^{-1} . Hydroxyl bending near this frequency is commonly encountered on metal oxides (63, 64). Overtones are likely to appear as the nearly harmonic potential well of this vibration is perturbed by adsorbed species (50). A band at this frequency has been observed in other studies of hydrated sulfated zirconia by Vedrine (12) and Morterra (42). In both instances, this band appeared at an intermediate stage of hydration and was obscured at higher degrees of hydration by the H–O–H scissors band at 1630 cm^{-1} . Morterra has given an alternate explanation for this absorbance by suggesting that water interacts directly with sulfate groups and does not hydrogen-bond with the surface. However, the heats of water adsorption on zirconia do not differ significantly from those of sulfated zirconia (54) and it is, therefore, likely that water interacts with the surface of zirconia that is not covered by sulfate groups. Further, the strengths of the heats of water adsorption on the catalyst dried at 773 K indicate dissociative adsorption (48, 49, 65).

The adsorption of water on sulfated zirconia after dehydration at 773 K produces hydroxyl groups that are not strongly acidic, as they do not contribute to the heat of ammonia adsorption, nor do they enhance adsorption of *n*-butane (54). A further study suggests that an important role of water on sulfated zirconia is to prevent the loss of water produced reversibly in the catalytic cycle (66). Overall, the maintenance of a certain degree of hydration on the surface of the sulfated zirconia catalyst is critical for *n*-butane isomerization.

CONCLUSIONS

The catalytic activity for a sample dried at 773 K is an order of magnitude lower compared to a sample dried at 588 K. Accordingly, a moderate degree of catalyst hydration is necessary for *n*-butane isomerization to occur over sulfated zirconia. The catalytic activity for the sample dried at 773 K is promoted by dosing quantities of water equal to approximately $75\text{ }\mu\text{mol/g}$ onto the surface at 423 K. At this level, the activity observed is approximately 70% of

the activity exhibited by sulfated zirconia dried at 588 K. Larger doses of water poison the catalyst.

Infrared spectroscopy indicates that the strongest acid sites on the catalyst dried at 588 K are almost entirely of the Brønsted acid type. Dehydration of the catalyst did not convert these sites into Lewis acid sites, nor did it alter their acid strength, as determined by microcalorimetric measurements of ammonia adsorption. Rehydration of the catalyst after drying at 773 K produces new hydroxyl groups that probably promote the isomerization reaction by preventing the loss of water produced reversibly in the catalytic cycle.

ACKNOWLEDGMENTS

This work was supported by funds provided by the Office of Basic Energy Sciences of the U.S. Department of Energy (DE-FG02-84ER13183). For providing graduate fellowships, we thank Amoco Oil Company (M.R.G.), Wisconsin Alumni Research Foundation (J.M.K.), and the National Defense Science and Engineering program (K.B.F.). We gratefully acknowledge the help of Robert Larson and Carolina Hartanto in conducting reaction kinetics experiments.

REFERENCES

1. Boesiger, D. D., Nielsen, R. H., and Albright, M. A. in "Encyclopedia of Chemical Technology" (H. F. Mark, Ed.), Vol. 12, p. 910. Wiley, New York, 1984.
2. Rossini, F. D., in "Physical Chemistry of the Hydrocarbons" (A. Farkas, Ed.), Vol. 1, ch. 1, p. 1950.
3. Pines, H., "The Chemistry of Catalytic Hydrocarbon Conversions." Academic Press, New York, 1981.
4. Hino, M., and Arata, K., *J. Chem. Soc. Chem. Commun.* 851 (1980).
5. Garin, F., Seyfried, L., Girard, P., Maire, G., Abdulsamad, A., and Sommer, J., *J. Catal.* **151**, 26 (1995).
6. Chen, F. R., Courdurier, G., Joly, J., and Vedrine, J. C., *J. Catal.* **143**, 616 (1993).
7. Riemer, T., Spielbauer, D., Hunger, M., Mekhemer, G. A. H., and Knözinger, H., *J. Chem. Soc. Chem. Commun.* 1181 (1994).
8. Lin, C. H., and Hsu, C. Y., *J. Chem. Soc. Chem. Commun.* 1479 (1992).
9. Garin, F., Seyfried, L., Girard, P., Maire, G., Abdulsamad, A., and Sommer, J., *J. Catal.* **151**, 26 (1995).
10. Bensitel, M., Saur, O., Lavalley, J. C., and Mabilon, G., *Mater. Chem. Phys.* **17**, 249 (1987).
11. Lunsford, J. H., Sang, H., Campbell, S. M., Liang, C., and Anthony, R. G., *Catal. Lett.* **27**, 305 (1994).
12. Babou, F., Courdurier, G., and Vedrine, J. C., *J. Catal.* **152**, 341 (1995).
13. Corma, A., Fornés, V., Juan-Rajadell, M. I., and López Nieto, J. M., *Appl. Catal. A* **116**, 151 (1994).
14. Comelli, R. A., Vera, C. R., and Parera, J. M., *J. Catal.* **151**, 96 (1995).
15. Pinna, F., Signoretto, M., Strukul, G., Cerrato, G., and Morterra, C., *Catal. Lett.* **26**, 339 (1994).
16. Morterra, C., Bolis, V., Cerrato, G., and Magnacca, G., *Surf. Sci.* **307-309**, 1206 (1994).
17. Nascimiento, P., Akrotopoulou, C., Oszagyan, M., Courdurier, G., Travers, C., Joly, J. F., and Vedrine, J. C. in "New Frontiers in Catalysis" (L. Guzzi, Ed.), Vol. 75, p. 1185. Elsevier, Amsterdam, 1993.
18. Zhang, C., Miranda, R., and Davis, B. H., *Catal. Lett.* **29**, 349 (1994).
19. Clearfield, A., Serrette, G. P. D., and Khazi-Syed, A. H., *Catal. Today* **20**, 295 (1994).
20. Mukaida, K., Miyoshi, T., and Satoh, T. in "Acid-Base Catalysis" (Tanabe, K., Hattori, H., Yamaguchi, T., and Tanaka, T., Eds.), p. 363. Kodansha, Tokyo, 1989.

21. Ward, D. A., and Ko, E. I., *J. Catal.* **150**, 18 (1994).
22. Morterra, C., Cerrato, G., and Bolis, V., *Catal. Today* **17**, 505 (1993).
23. Arata, K., *Adv. Catal.* **37**, 165 (1990).
24. Davis, B. H., Keogh, R. A., and Srinivasan, R., *Catal. Today* **20**, 219 (1994).
25. Corma, A., Martínez, A., and Martínez, C., *J. Catal.* **149**, 52 (1994).
26. Yamaguchi, T., *Appl. Catal.* **61**, 1 (1990).
27. Navío, J. A., Macías, M., Real, C., and Colón, G., *Mater. Lett.* **20**, 345 (1994).
28. Norman, C. J., Goulding, P. A., and McAlpine, I., *Catal. Today* **20**, 313 (1994).
29. Escalona Platero, E., and Peñarroya Mentrut, M., *Catal. Lett.* **30**, 31 (1995).
30. Morterra, C., Cerrato, G., Pinna, F., Signoretto, M., and Strukul, G., *J. Catal.* **149**, 181 (1994).
31. Keogh, R. A., Srinivasan, R., and Davis, B. H., *J. Catal.* **151**, 292 (1995).
32. Handy, B. E., Sharma, S. B., Spiewak, B. E., and Dumesic, J. A., *Meas. Sci. Technol.* **4**, 1350 (1993).
33. Kobe, J. M., Fogash, K. B., González, M. R., and Dumesic, J. A., in progress (1996).
34. Yori, J. C., Luy, J. C., and Parera, J. M., *Appl. Catal.* **46**, 103 (1989).
35. Ng, F. T. T., and Horvát, N., *Appl. Catal. A* **123**, L197 (1995).
36. Kobe, J. M., González, M. R., Fogash, K. B., and Dumesic, J. A., in preparation (1996).
37. Adeeva, V., de Haan, J. W., Jänchen, J., Lei, G. D., Schünemann, V., van de Ven, L. J. M., Sachtler, W. M. H., and van Santen, R. A., *J. Catal.* **151**, 364 (1995).
38. Bensitel, M., Saur, O., Lavalley, J. C., and Morrow, B. A., *Mater. Chem. Phys.* **19**, 147 (1988).
39. Nakamoto, K., "Infrared and Raman Spectra of Inorganic and Coordination Compounds." Wiley-Interscience, New York, 1986.
40. Yamaguchi, T., Jin, T., and Tanabe, K., *J. Phys. Chem.* **90**, 3148 (1985).
41. Horn, W. R., Weissberger, E., and Collman, J. P., *Inorg. Chem.* **9**, 2367 (1970).
42. Morterra, C., Cerrato, G., Pinna, F., and Signoretto, M., *J. Phys. Chem.* **98**, 12373 (1994).
43. Little, L. H., "Infrared Spectra of Adsorbed Species." Academic Press, New York, 1966.
44. Kustov, L. M., Kazansky, V. B., Figueras, F., and Tichit, D., *J. Catal.* **150**, 143 (1994).
45. Fogash, K. B., Yaluris, G., González, M. R., Ouraipryvan, P., Ward, D. A., Ko, E. I., and Dumesic, J. A., *Catal. Lett.* **32**, 241 (1995).
46. Yaluris, G., Larson, R. B., Kobe, J. M., González, M. R., Fogash, K. B., and Dumesic, J. A., *J. Catal.* **158**, (1996).
47. Spiewak, B. E., Handy, B. E., Sharma, S. B., and Dumesic, J. A., *Catal. Lett.* **23**, 207 (1994).
48. Coster, D. J., Fripiat, J. J., Muscas, M., and Auroux, A., *Langmuir* **11**, 2615 (1995).
49. Romanovskii, B. V., Topchieva, K. V., Stolyarova, L. V., and Alekseev, A. M., *Kinet. Katal.* **11**, 1525 (1969).
50. Flygare, W. H., "Molecular Structure and Dynamics." Prentice-Hall, Englewood Cliffs, NJ, 1978.
51. Hindin, S. G., Oblad, A. G., and Mills, G. A., *J. Am. Chem. Soc.* **77**, 535 (1955).
52. Haldeman, R. G., and Emmett, P. H., *J. Am. Chem. Soc.* **78**, 2922 (1956).
53. MacIver, D. S., Emmett, P. H., and Frank, H. S., *J. Phys. Chem.* **62**, 934 (1958).
54. Fogash, K. B., González, M. R., Kobe, J. M., and Dumesic, J. A., in progress (1996).
55. Cardona-Martínez, N., and Dumesic, J. A., *J. Catal.* **128**, 23 (1991).
56. Parrillo, D. J., Gorte, R. J., and Farneth, W. E., *J. Am. Chem. Soc.* **115**, 12441 (1993).
57. Parrillo, D. J., Lee, C., Gorte, R. J., White, D., and Farneth, W. E., *J. Phys. Chem.* **99**, 8745 (1995).
58. Cheung, T. K., d'Itri, J. L., and Gates, B. C., *J. Catal.* **153**, 344 (1995).
59. Sikabwe, E. C., Coelho, M. A., Resasco, D. E., and White, R. L., *Catal. Lett.* **34**, 25 (1995).
60. Jatia, A., Chang, C., MacLeod, J. D., Okubo, T., and Davis, M. E., *Catal. Lett.* **25**, 21 (1994).
61. Ghenciu, A., Li, J. Q., and Farcasiu, D., presented at 14th North American Meeting of the Catalysis Society, Snowbird, Utah, 1995.
62. González, M. R., Ph.D. dissertation, University of Wisconsin—Madison (1995).
63. Bellamy, L. J., "The Infrared Spectra of Complex Molecules." Chapman and Hall, New York, 1980.
64. Lavalley, J. C., Bensitel, M., Gallas, J. P., Lamotte, J., Busca, G., and Lorenzelli, V., *J. Mol. Struct.* **175**, 453 (1988).
65. Fubini, B., Bolis, V., Bailes, M., and Stone, F. S., *Solid State Ionics* **32/33**, 258 (1989).
66. Fogash, K. B., Larson, R. B., Gonzalez, M. R., Kobe, J. M., and Dumesic, J. A., submitted for publication (1996).